

Regulation of Cell Adhesion on Physically Crosslinked Hydrogels Composed of Amino Acid-Based Polymers by Changing Elastic Modulus Using Shape Fix/Memory Properties

Shin-nosuke Nishimura,* Tomoya Yoshida, Nobuyuki Higashi, and Tomoyuki Koga*

The elastic modulus of hydrogels is one of the most important factors for controlling cell fate. In this study, hydrogels composed of poly(*N*-acryloylglycinamide) (PNAGAm) grafted with arginine (R)-glycine (G)-aspartic acid (D)-serine (S) peptide is designed without a chemical crosslinker. The hydrogels are prepared by the conventional radical copolymerization of *N*-acryloylglycinamide with a polymerizable RGDS peptide. The peptide grafting ratio is easily controlled by adjusting the feed composition for polymerization. The hydrogels exhibit thermo-responsiveness of the upper critical solution temperature type based on the PNAGAm moiety. This characteristic reflects the shape fix/memory properties of hydrogels because of the reversible formation of multiple hydrogen bonds. The cell adhesiveness of the hydrogels drastically improves in the presence of a small amount of the peptide graft. The hydrogels exhibit good biocompatibility; the adhered cells proliferate on the hydrogels, and macrophages do not show activation or inflammation. Surfaces with different elastic modulus regions are successfully constructed on the same hydrogel by using shape fix/memory properties, allowing the regulation of cell adhesion. This hydrogel system offers promising opportunities for the design and application of functional cell scaffolds.

1. Introduction

Cells in the natural environment are surrounded by a scaffold composed of an extracellular matrix that supports cell growth through adhesion, proliferation, and differentiation. Artificial scaffold materials are required when cells are cultured *in vitro*. Significant efforts are made to develop biomaterials for tissue engineering and regenerative medicine, which are attractive techniques for developing functional substitutes for damaged tissues.^[1–5] Hydrogels, in which polymer chains are

chemically and/or physically crosslinked, show considerable potential in biomedical applications because of their high water content, biocompatibility, and consistency similar to that of soft tissue.^[6–9] Therefore, hydrogels have been investigated as desirable scaffold materials for controlling various aspects of cellular behavior.^[10,11] Cell behaviors, including adhesion, proliferation, and differentiation, are affected by various scaffold properties, such as surface roughness,^[12–17] hydration state,^[17–22] and elastic modulus.^[23–30] Elastic modulus of hydrogels is one of the most preferable factors for controlling the fate of cells because it can be readily changed by easy manipulation. In general, a chemically crosslinked hydrogel, represented by the polyacrylamide/*N,N'*-methylenebis(acrylamide) system, is preferably used to construct scaffolds with different elastic moduli. However, to control elasticities of the hydrogels, the feed composition of main monomer and

crosslinking agent should be changed. This results in a difference in the copolymer composition between softer and harder hydrogels. Consequently, not only the elasticity but also various characteristics of the hydrogels, including the hydrophilicity/hydrophobicity balance, are simultaneously altered. This leads to difficulties in discussing the specific effects of the hydrogels' elasticity on cell behaviors on their surfaces. Therefore, a novel hydrogel system has been desired to prepare distinct regions with different elastic moduli from an identical hydrogel without specific chemical treatments.

We focused on poly(*N*-acryloylglycinamide) (PNAGAm) as the base polymer for constructing cell scaffolds with different elastic moduli. PNAGAm is an amino acid-derived vinyl polymer whose side chains exhibit strong hydrogen bonds between the polymer chains. The polymer is expected to form a hydrogel without a chemical crosslinker at concentrations >2% and is both biocompatible and biodegradable.^[31,32] Our previous study clarified that chemically crosslinked PNAGAm hydrogels exhibit excellent mechanical toughness based on the cooperative interplay of two distinct chemical and physical cross-linkages

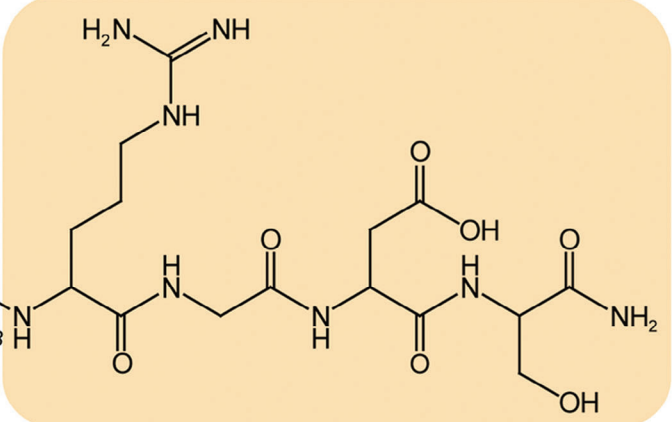
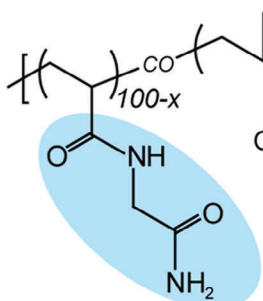
S.-n. Nishimura, T. Yoshida, N. Higashi, T. Koga
Department of Molecular Chemistry and Biochemistry
Faculty of Science and Engineering
Doshisha University
1–3 Tatara Miyakodani, Kyotanabe, Kyoto 610-0394, Japan
E-mail: shnshim@mail.doshisha.ac.jp; tkoga@mail.doshisha.ac.jp

 The ORCID identification number(s) for the author(s) of this article can be found under <https://doi.org/10.1002/admt.202301598>

DOI: 10.1002/admt.202301598

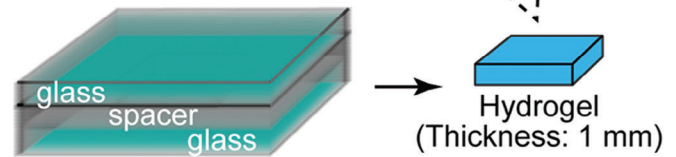
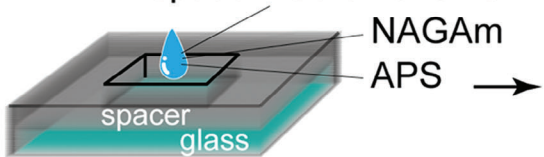
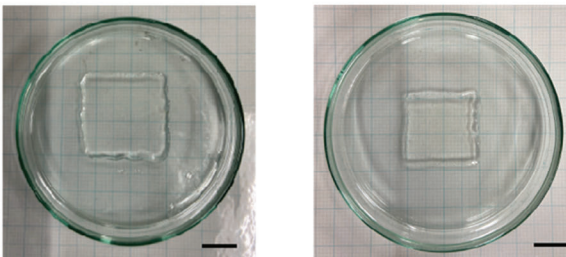
A

NAGAm units
Thermo-responsiveness
Shape fix/memory property

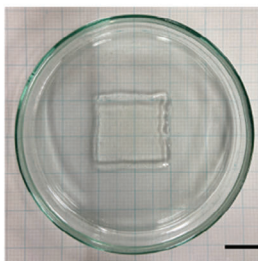


RGDS peptide units
Cell adhesiveness

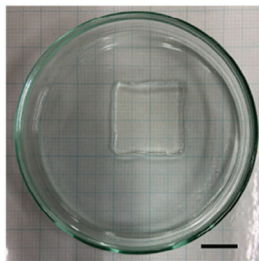
Peptide-macromonomer

**B**

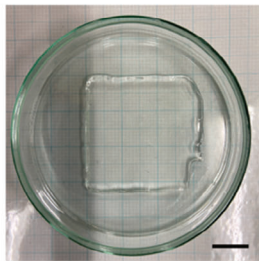
grafting ratio (x) = 0%
(PNAGAm)



$x = 1\%$



$x = 2\%$



$x = 5\%$

Figure 1. Preparation of the hydrogels composed of RGDS peptide-grafted PNAGAm. A) Schematic of the hydrogels by radical copolymerization of NAGAm with the peptide macromonomer. B) Photographs of the hydrogels with various grafting ratios of the peptide. Scale bar is 1 cm.

and exhibit shape fix/memory functions based on the thermo-reversible formation of hydrogen bonds (upper critical solution temperature (UCST)-type).^[33] Based on this, we anticipated that the PNAGAm hydrogel would possess shape fix/memory properties without a particular chemical crosslinker in a practical temperature range for biomedical applications and enable the construction of different elastic moduli using these properties.

However, most hydrogels do not allow cells to adhere to their surface. Chemically synthesized short arginine–glycine–aspartic acid (RGD) and RGD-serine (RGDS) peptides, which are the principal integrin-binding domains of fibronectin, are often used to improve the adhesion of scaffolds in tissue engineering.^[34–37] We previously reported that the cell adhesiveness of a poly(2-

hydroxyethyl methacrylate) hydrogel, which resists the nonspecific adhesion of cells, is drastically improved by hybridization with a small amount of the RGDS peptide.^[38–40] In this study, hydrogels of RGDS peptide-grafted PNAGAm without chemical cross-linkage were designed and prepared from an amino acid-derived composition. The hydrogels were prepared by the conventional radical copolymerization of *N*-acryloylglycinamide (NAGAm) with a polymerizable RGDS peptide (Figure 1A). The characteristics of the hydrogels were evaluated, and their cell adhesion behavior onto the hydrogels was studied in detail. In addition, we demonstrated the successful construction of three distinct surfaces with different elastic moduli on the same hydrogel, utilizing shape fix/memory properties, and evaluated cell adhesion behaviors on the surfaces.

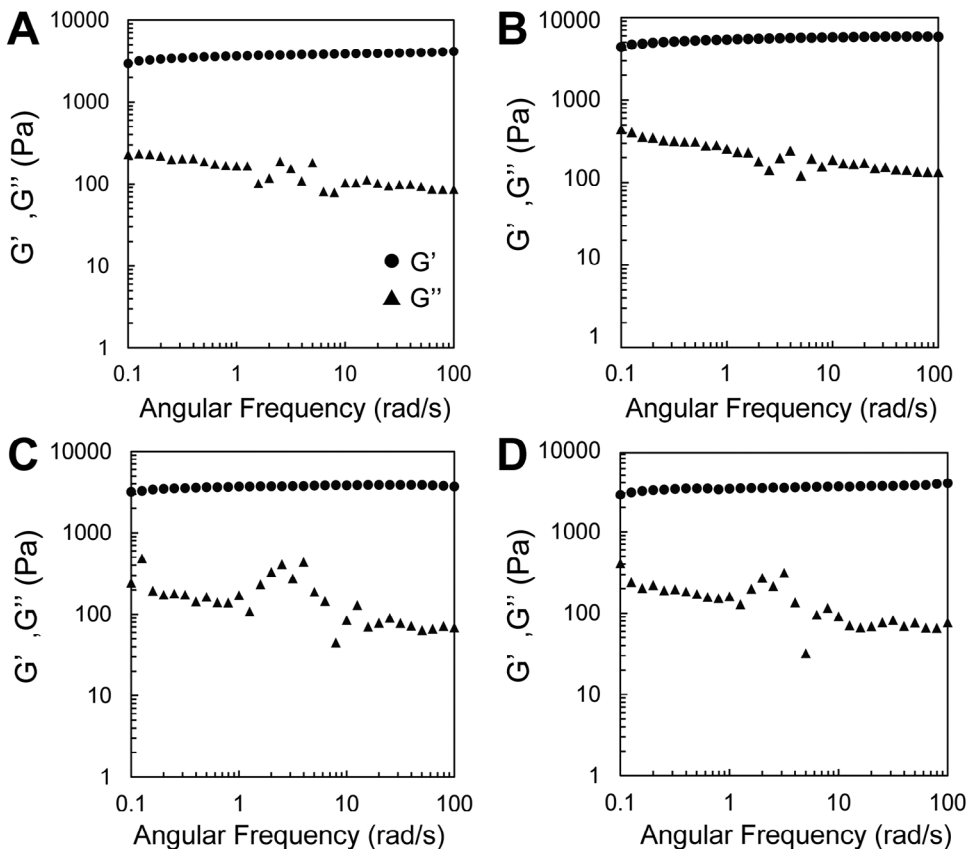


Figure 2. Rheology analyses for the hydrogels at 37 °C. The grafting ratios are A) $x = 0\%$, B) 1% , C) 2% , and D) 5% , respectively. The storage moduli (G') (circle) and loss moduli (G'') (triangle) of the hydrogels are plotted as a function of frequency ($0.1\text{--}100\text{ rad s}^{-1}$) at 1% strain.

2. Results and Discussion

2.1. Preparation of Hydrogel Composed of RGDS Peptide-Grafted PNAGAm

NAGAm was synthesized according to our previous report,^[33] and its structure was confirmed by ^1H NMR spectroscopy (Figure S1, Supporting Information). The polymerizable RGDS peptide (methacryloyl-GGGRGDS-Am) was synthesized by solid-phase peptide synthesis using 9-fluorenylmethoxycarbonyl (Fmoc) chemistry, which was acylated by methacrylic anhydride at *N*-terminus to allow radical copolymerization with NAGAm and amidated at *C*-terminus to ignore the end group effect. All coupling reactions involved in preparing the target peptide segment were performed on the resin. The peptide was cleaved from the resin by treatment with trifluoroacetic acid and identified using matrix-assisted laser desorption/ionization time-of-flight (MALDI-TOF) mass spectrometry and ^1H NMR spectroscopy (Figure S2, Supporting Information).

Hydrogels composed of PNAGAm and RGDS peptides were prepared by copolymerization of NAGAm with the peptide macromonomer under various feed compositions (grafting ratio (x) = 0%, 1%, 2%, and 5%) (Figure 1A). An aqueous solution containing the monomers and 1 mol% ammonium persulfate (APS) as a radical initiator (final monomer concentration of 1 M) was sandwiched between two glass plates with a silicon

spacer (W: 30 mm, D: 30 mm, H: 1 mm) and heated at 70 °C for 16 h. The NAGAm units formed strong hydrogen bonds acting as physical crosslinks between the polymer chains; therefore, the mixture became a hydrogel with progressive copolymerization (Figure 1B). Note that the monomer conversions in the polymerization systems were determined to be over 99% through ^1H NMR spectroscopy and the grafting ratios agreed with the feed compositions of the peptide macromonomer. These hydrogels were sufficiently transparent and self-supporting in fresh pure water at ambient temperature regardless of the existence of the peptide grafts although the hydrogels shrank at this temperature compared with 70 °C based on the thermo-responsivity of the NAGAm units. In the case of $x = 5\%$, the shrinkage ratio of the hydrogel was smaller than that of the others because the hydrophilic peptide grafts promoted the hydration of the polymer chains.

To evaluate the elasticity of the hydrogels soaked in phosphate-buffered saline without calcium and magnesium ions (PBS (-)), rheological analyses were performed at 37 °C. Figure 2 shows the storage (G') and loss (G'') moduli changes of the hydrogels depending on frequency. The values of G' for all hydrogels were nearly constant and consistently higher than the G'' values at all frequencies, indicating that the hydrogels possess stable crosslinking points. At the frequency of 6.3 rad s^{-1} , the G' values were 3710 ($x = 0$), 3700 ($x = 1$), 3700 ($x = 2$), and 3500 Pa ($x = 5$). These results suggested that the peptide grafts had little impact

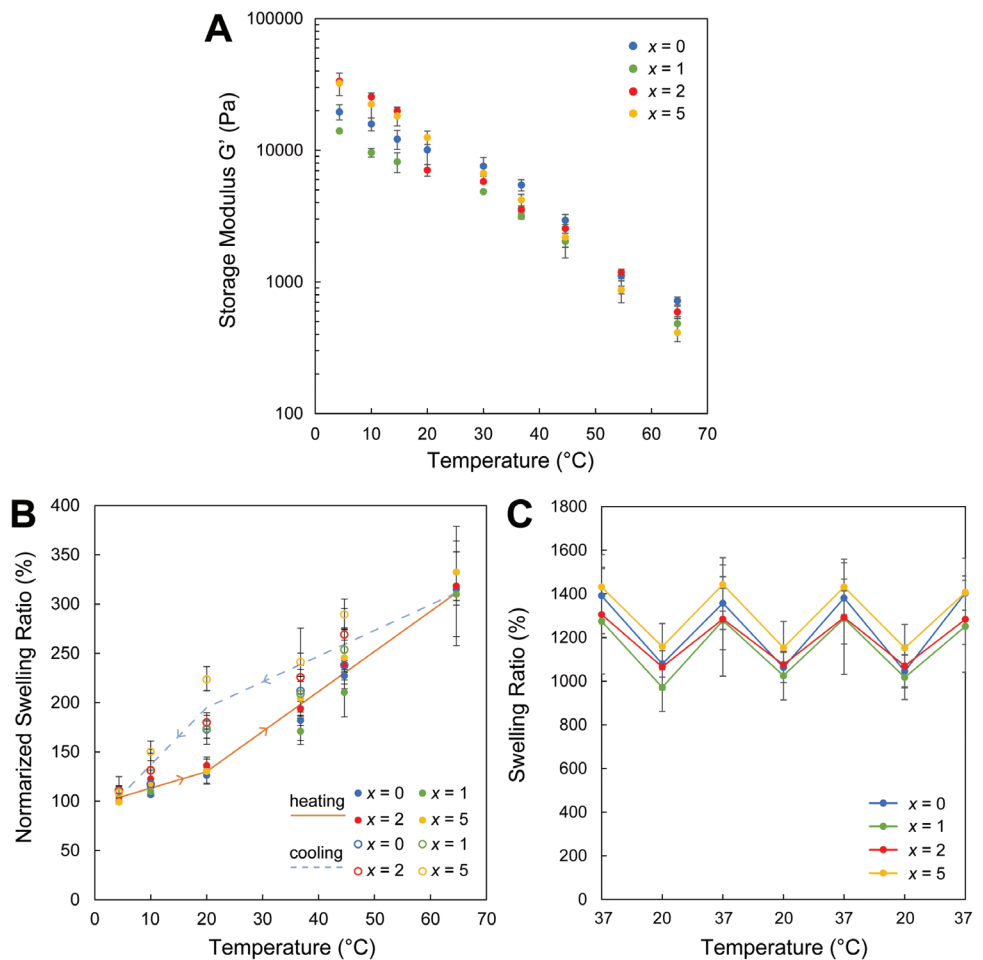


Figure 3. Evaluation for thermo-responsiveness of the hydrogels. A) Temperature dependence of the G' values of the hydrogels at 6.3 rad s^{-1} (1% strain). B) Normalized swelling ratio of the hydrogels between 4 and 65 °C. The values were normalized to 100% at 4 °C in the heating processes. C) Reversible changes in the swelling ratio of the hydrogels at 20 and 37 °C.

on the elastic moduli of the hydrogels. Thus, PNAGAm-based hydrogels were successfully prepared with different amounts of the RGDS peptide and sufficient strength for cell experiments.

2.2. Thermo-Responsive Behaviors and Shape Memory/Fix Property of the Hydrogels

The main component of the hydrogels is the NAGAm unit, of which homopolymer exhibits thermo-responsiveness of the UCST-type. This behavior is based on the reversible formation of hydrogen bonds, which cause changes in the crosslinking density and spreading of polymer chains in the hydrogels. We previously reported that chemically crosslinked hydrogels of the NAGAm homopolymer show reversible swelling and shrinking behavior upon thermal stimulation.^[33] To investigate the influence of peptide grafts on thermo-responsiveness of the physically crosslinked hydrogels prepared in this study, G' values of the hydrogels were measured at different temperatures (4, 10, 15, 20, 30, 37, 45, 55, and 65 °C) while maintaining a constant frequency of 6.3 rad s^{-1} (Figure 3A). The hydrogels were soaked in phosphate-buffered saline (PBS) (–) before the experiments.

All hydrogels exhibited a consistent decrease in the G' values as the temperature increased. Particularly, at 65 °C, the G' values were approximately one-hundredth to one-fiftieth of the values observed at 4 °C because the hydrogen bonds between the polymer chains are partly disrupted, reducing the crosslinking density.

The changes in the elastic modulus in response to the thermo-responsiveness of the polymers were closely related to the swelling and shrinking behaviors of the hydrogels. Figure 3B shows swelling ratio changes as a function of temperature, of which values were normalized to 100% at 4 °C in the heating process. All hydrogels swelled with increasing temperature, and their swelling ratios reached 300%, regardless of the presence of peptide grafts. During the cooling process, the swelling ratios of the hydrogels returned to their original values with slight hysteresis. This hysteresis suggests that reversible structural changes or rearrangement of the polymer chains might have occurred within the hydrogel network owing to the formation and breakage of hydrogen bonds during the swelling and shrinking processes in response to temperature variations. Such swelling–shrinking behaviors were also caused reversibly by a narrow temperature change between 20 and 37 °C (Figure 3C). Thus, hydrogels are

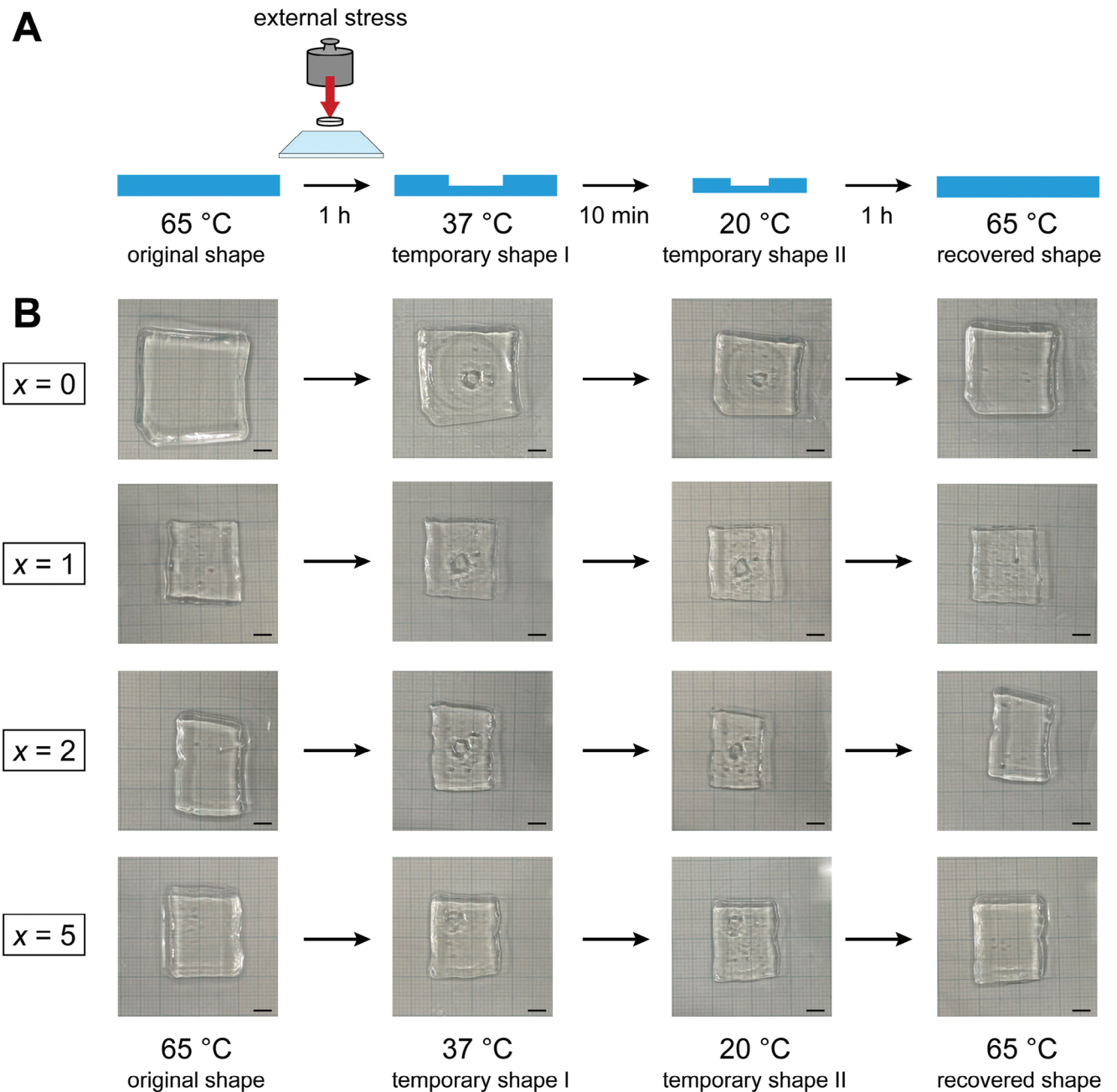


Figure 4. A) Schematic of the shape fix/memory experiments for the hydrogels. B) Photographs of the hydrogels at each step. Scale bar is 1 cm.

highly responsive to small changes in temperature, making them suitable candidates for bioapplications at physiological temperatures.

We studied the shape fix/memory properties of the hydrogel by the reversible formation of hydrogen bonds in response to the thermal stimulus according to the process shown in Figure 4A. Figure 4B shows the photographs of the hydrogels at each step of the experiment. Initially, the original hydrogels were heated to 65 °C in PBS (–) to induce the partial breakdown of hydrogen bonds. The hydrogels did not undergo erosion, even in the presence of a large amount of water. Subsequently, the hydrogels

were pressed with a polystyrene tip ($\phi 5$ mm) by applying external stress with a weight of 100 g (≈ 50 kPa) while maintaining the temperature at 65 °C for 1 h. Both the hydrogels and weights were then immersed in PBS (–) at 37 °C and incubated at the same temperature for 1 h to allow for the formation of hydrogen bonds. Even after removing the weight, all hydrogels still exhibited a ≈ 4 mm dent on their surfaces (temporal shape I). This is important because hydrogels can maintain their fixed shape at the cell culture temperature. After cooling to 20 °C, the dents did not disappear, although they became smaller because of the shrinking of the hydrogels (temporary shape II) (Figure S3, Supporting

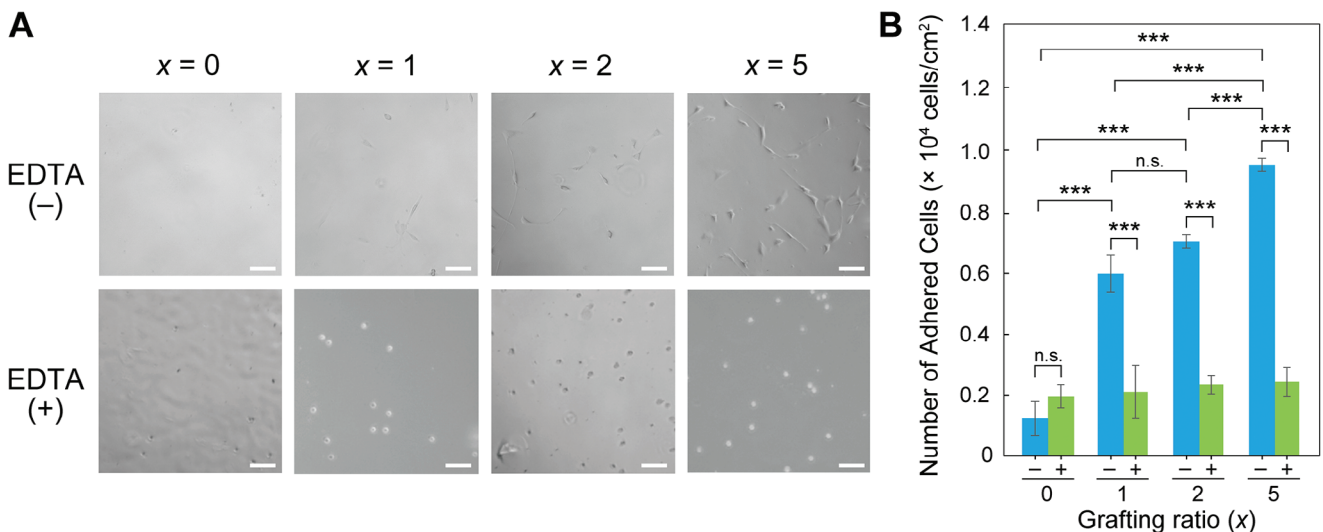


Figure 5. Cell adhesion behaviors of NIH/3T3 cells onto the hydrogels cultured for 16 h in the serum-free medium without (−) and with (+) 5 mM EDTA. A) Phase contrast images of the adhered cells. B) Number of the adhered cells was calculated by WST-8 assay. Statistical analysis was performed using the t-test ($N = 3$). Error bars represent the standard deviation. *** $p < 0.005$; n.s., not significant.

Information). However, the hydrogels with temporary shape II were completely returned to the original state by heating at 65 °C (recovered shape). This demonstrates that the hydrogels possessed shape fix/memory properties based on the reversible formation of hydrogen bonds. We have previously reported that the importance of hydrogen bonds in the shape/fix memory behaviors of chemically crosslinked-PNAGAm. Indeed, the addition of urea, a well-known hydrogen bond breaker, resulted in the weakening of hydrogen bonds within the PNAGAm network.^[33,41] From these results, we concluded that the RGDS peptide-grafted PNAGAm hydrogels possess shape fix/memory capability even in the presence of peptide grafts, enabling them to retain their temporary shape even at the cell culturing temperature.

2.3. Effect of the RGDS-Peptide Grafts for Cell Adhesion Behaviors on the Hydrogels

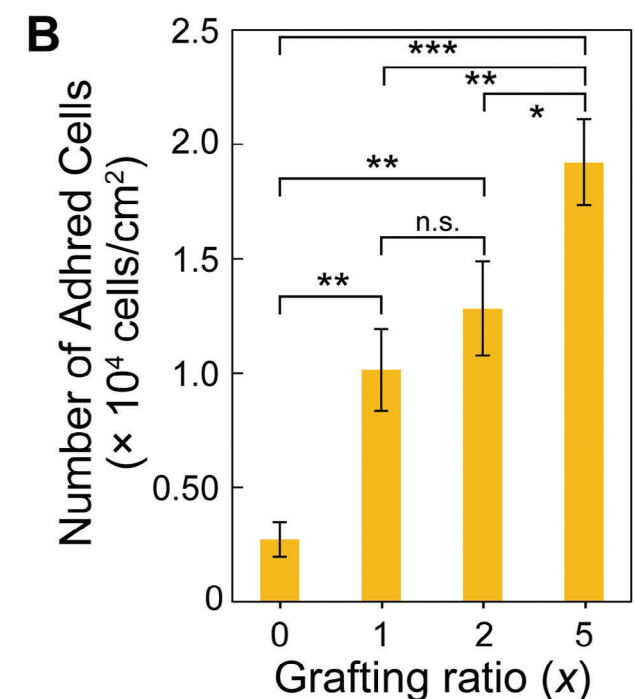
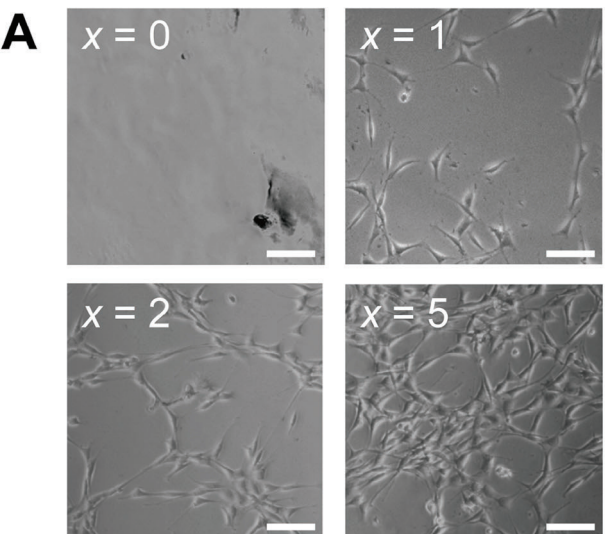
The ability of PNAGAm hydrogels with RGDS peptide grafts for cell adhesion was confirmed using a mouse embryo fibroblast cell line (NIH/3T3) (Figure 5). The NIH/3T3 cells (3.0×10^4 cells cm^{-2}) were first seeded onto the hydrogels in a serum-free medium without (−) ethylenediaminetetraacetic acid (EDTA) and cultured at 37 °C for 16 h. Figure 5A (tops) shows phase contrast images of the adhered cells on the hydrogels. Negligible adhesion was observed on the hydrogel without peptide grafts ($x = 0$). By contrast, many adherent cells were clearly observed on the peptide-grafted hydrogels ($x = 1, 2$, and 5), and these cells exhibited a well-extended morphology. These results strongly indicate that the presence of RGDS-peptide grafts significantly promoted cell adhesion to the PNAGAm hydrogels. These experiments were quantified using the WST-8 assay, as shown in Figure 5B (blue bars). The number of adhered cells on the peptide-grafted hydrogels was notably higher than that on the PNAGAm homopolymer hydrogel (six-ten times, $p < 0.005$). Moreover, an increase in the grafting ratio of the RGDS peptide

further enhanced cell adhesion, demonstrating the positive effect of RGDS grafts on cell attachment. Similar experiments were conducted in the presence of 5 mM EDTA (+) to validate the effect of RGDS grafts on cell adhesion in the hydrogels. EDTA removes divalent cations such as Ca^{2+} and Mg^{2+} from their binding sites, thereby inhibiting integrin-ligand interactions.^[42,43] The number of adhered cells drastically decreased and was hardly observed on any hydrogels (Figure 5A, bottom). The number of adhered cells on the RGDS peptide-grafted hydrogels significantly reduced to the same level as that on the PNAGAm homopolymer hydrogel (Figure 5B, green bars). From these results, we concluded that the enhanced cell adhesion onto the peptide-grafted hydrogels was attributed to the presence of peptide grafts and the cells adhered through integrin-ligand interactions.

Serum proteins, including fibronectin and vitronectin, coexist in cell culture systems. We evaluated the cell adhesion behavior onto the hydrogels in a serum medium to confirm the effect of the RGDS-peptide grafts (Figure 6). The NIH/3T3 cells (3.0×10^4 cells cm^{-2}) were seeded onto the hydrogels and cultured at 37 °C for 16 h. Figure 6A shows phase contrast images of the adhered cells on the hydrogels. Similar to the results under serum-free conditions, the peptide-grafted hydrogels promoted the adhesion of cells compared to the hydrogel of the PNAGAm homopolymer ($x = 0$). The number of adhered cells on the peptide-grafted hydrogel was higher than that on the PNAGAm homopolymer hydrogel (four-nine times, $p < 0.01$) (Figure 6B). These results indicated that the peptide-grafted hydrogels effectively functioned as a cell scaffold in the presence of serum.

2.4. Biocompatibility Test for the Peptide-Grafted Hydrogels

Cell scaffolds constructed from artificial polymers often exhibit cytotoxicity, even if they allow initial cell adhesion within a brief period. To assess the biocompatibility of the RGDS



peptide-grafted hydrogels, we studied the proliferative behavior of adhered cells on the hydrogels in a serum medium. Figure 7A shows the growth curve for the NIH/3T3 cells on the various hydrogels over 10 d (seeding density: 2.0×10^3 cells cm^{-2}). The trend of the initial cell adhesion (1 d) was consistent with the results of the cell adhesion experiments. Throughout the first 5 d, significant logarithmic proliferation of adhered cells was observed on all hydrogels. The rate of cell proliferation varied

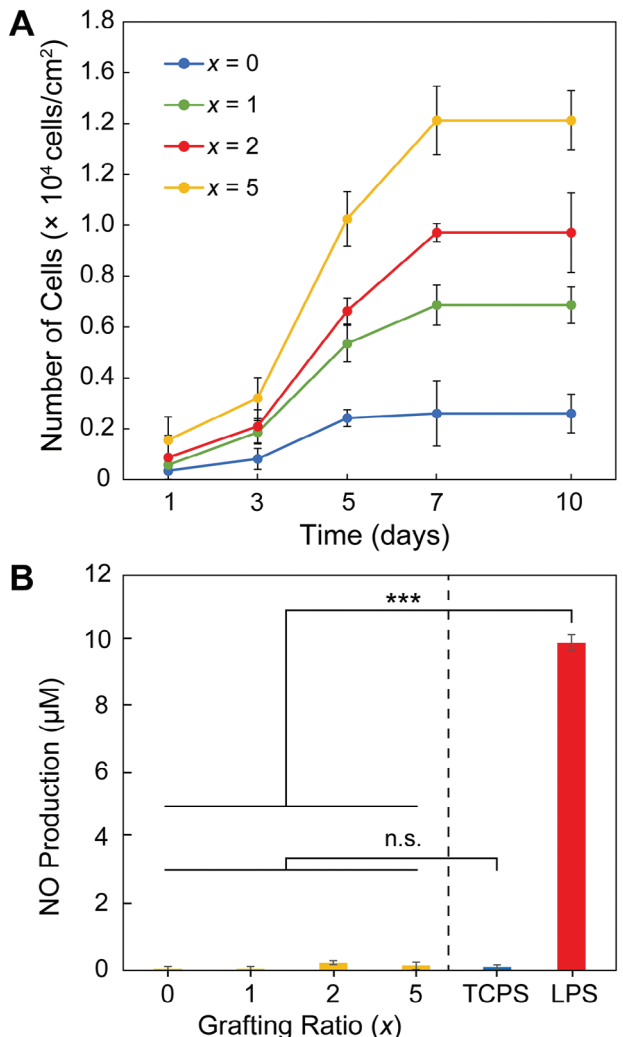


Figure 7. Biocompatibility test for the hydrogels. A) Proliferation behaviors of the adhered NIH/3T3 cells on the hydrogels. The number of adhered cells was calculated by the WST-8 assay. Error bars represent the standard deviation ($N = 3$). B) Summary of NO production from the adhered RAW264.7 cells on the hydrogels. The same experiments were also performed on TCPS, with LPS (1 ng mL^{-1}) as a positive control and without LPS as a negative control. Statistical analysis was performed using the t-test ($N = 3$). Error bars represent the standard deviation. *** $p < 0.005$; n.s., not significant.

depending on the number of peptide grafts present in the hydrogels. At day 10, the number of cells on the peptide-grafted hydrogels increased by $\approx 9\text{--}10$ times compared to the cell count at day 1 whereas the increase in the PNAGAm homopolymer hydrogel was limited to approximately five times. The cells that adhered to the peptide-grafted hydrogels formed a confluent layer, although the absolute cell counts varied owing to differences in cell extension. These results suggested that the peptide-grafted hydrogels did not exhibit cytotoxicity and interrupted cell growth. The amount of the peptide affected the adhesion force of the cells on the hydrogels. PNAGAm-based hydrogels undergo shrinkage in response to decreases in temperature. After culturing the cells for 10 d, the peptide-grafted hydrogels were soaked into a

serum medium at 25 °C. The cells easily detached as a cell sheet from the hydrogel with $x = 1$, whereas they remained adhered to hydrogels with $x = 2$ and 5 (Figure S4A,B, Supporting Information). Thus, by controlling the grafting ratio, our hydrogels can serve as scaffolds for both cell culture and cell sheet preparation.

The potential stimulatory effects of scaffolds, such as the activation of inflammatory signaling, are a significant concern in the design of biomaterials for *in vivo* applications. Macrophages, including mouse macrophage-like cells (RAW264.7), generate nitric oxide (NO) in response to stimulating agents such as lipopolysaccharide (LPS).^[44] Cellular production of NO serves as an indicator of the stimulatory effects of polymers in activating macrophages and eliciting an inflammatory response within cells. To investigate the biocompatibility of the hydrogels in detail, the RAW264.7 cells (1.0×10^6 cells cm^{-2}) were cultured on the hydrogels for 24 h at 37 °C, and then NO production in the adhered cells was measured (Figure 7B). The RAW264.7 cells were also cultured on tissue culture polystyrene (TCPS), with LPS (1 ng mL^{-1}) as the positive control and without LPS as the negative control. The strong adhesiveness of the RAW264.7 cells resulted in their attachment to the hydrogels, irrespective of the presence of peptide grafts (Figure S5, Supporting Information). NO production by cells adhered to the PNAGAm-based hydrogels was at the same level as that observed on TCPS, resulting in negligible stimulatory and inflammatory effects on macrophages. From these results, we conclude that PNAGAm-based hydrogels with and without peptide grafts have superior biocompatibility and significant potential for use as cell scaffold materials.

2.5. Control of Cell Adhesion Behaviors onto the Hydrogels Using the Shape Fix Property

The behavior of cells adhering to hydrogel scaffolds is affected by the elastic modulus of the scaffold.^[23–29] The peptide-grafted PNAGAm synthesized in this study showed hydrogel formation and shape fix/memory properties based on reversible hydrogen bonding. If the thickness of the hydrogel could be changed site-specifically from an initially identical thickness by compression and shape fixation while maintaining the same aspect ratio, the elastic modulus of the hydrogels could also be controlled owing to changes in the density of the polymer network and/or hydrogen bond-based crosslinks.

We designed and fabricated a device using the 3D printer shown in Figure S6 (Supporting Information), which could apply a uniform force to push a hydrogel (1 × 3 cm) and constructed three distinct regions (1 × 1 cm each) with different thicknesses. This device could simultaneously process three hydrogels. For this experiment, we used a peptide-grafted hydrogel ($x = 2$) because of its sufficient RGDS peptide content to maintain stable cell adhesion. A hydrogel with $x = 2$ (1 × 3 cm) was placed on the device and pressed (≈ 50 kPa) while maintaining the temperature at 65 °C for 1 h. The device, including the hydrogel, was cooled to 37 °C and incubated at the same temperature for 1 h for shape-fixation of the hydrogel based on the re-formation of the hydrogen bond. Figure 8A shows the photographs of the hydrogels after treatment: (i) non-pressed, (ii) moderately pressed, and (iii) firmly pressed regions. The hydrogel was clearly fixed, and the thicknesses of each region were 1.0 (i), 0.64 (ii), and 0.50 mm (iii).

Rheological analyses were performed to evaluate the elasticity of each region (Figure 8B). Each sample exhibits a constant elastic modulus (no significant difference) over the frequency range of 0.1–100 rad s^{-1} , and the G' values at the frequency of 6.3 rad s^{-1} were 3460 (i), 5940 (ii), and 9460 Pa (iii). Hence, the elastic modulus of the hydrogel was successfully altered by the shape-fix property without modifying its chemical components.

Subsequently, we demonstrated cell adhesion to shape-fixed hydrogels. The NIH/3T3 cells (3.0×10^4 cells cm^{-2}) were seeded onto the hydrogels in serum medium and cultured at 37 °C for 16 h. Figure 8C shows phase contrast images for the adhered cells in each region. Numerous adherent cells were observed in all regions, although the cell morphologies were slightly different. In the softest region (i), the morphology of the adhered cells was flat, and some of the cells were relatively rounded. By increasing the elastic modulus of the hydrogel, the adhered cells were extended, and their morphologies were elongated in the hardest region (iii). The morphology of fibroblasts is round on soft gels and well extent on stiff gels.^[23] In addition, the number of adhered cells increased with an increase in the elastic modulus of the hydrogel and was 1.3×10^4 cells cm^{-2} (i), 1.6×10^4 cells cm^{-2} (ii), and 1.9×10^4 cells cm^{-2} (iii) (Figure 8D). Thus, we succeeded in preparing hydrogels with different elastic moduli by using shape fix/memory properties, whose surfaces enable control of cell adhesion and extension behaviors. This knowledge offers a promising opportunity for the design and application of novel cell scaffold materials.

3. Conclusion

In this study, we prepared RGDS peptide-grafted PNAGAm hydrogels synthesized from amino acid-derived components and evaluated the characteristics of the hydrogels, including their cell adhesion behavior. The hydrogels were transparent and self-supported at various temperatures. The values of G' for the hydrogels at 37 °C were approximately the same, regardless of the presence of peptide grafts. Although the elastic modulus and swelling ratio of the hydrogels responded to the thermal stimulus based on the UCST behavior, the hydrogels did not dissolve in water. Using USCT behavior, the hydrogels displayed shape fix/memory properties based on the partial breakdown and reformation of hydrogen bonds, of which the temporary shapes were maintained even at the cell culturing temperature. The peptide grafts clearly improved the cell adhesiveness of the hydrogels for NIH/3T3 cells, and the number of adhered cells increased with increasing grafting ratio. The hydrogels had superior biocompatibility because the adhered NIH/3T3 cells proliferated, and RAW264.7 cells showed negligible NO production. Surfaces with different elastic moduli composed of the same hydrogel were successfully constructed by utilizing shape fix/memory properties, in which the NIH/3T3 cells showed different adhesion behaviors. Thus, hydrogels composed of PNAGAm with the RGDS peptide can be used not only as simple cell scaffolds but also as functional scaffolds for controlling cell behavior. These attractive characteristics differentiate this system from conventional hydrogel systems. We believe the hydrogel system using the RGDS peptide-grafted PNAGAm has significant potential and offers a promising opportunity for designing and applying functional cell scaffolds.

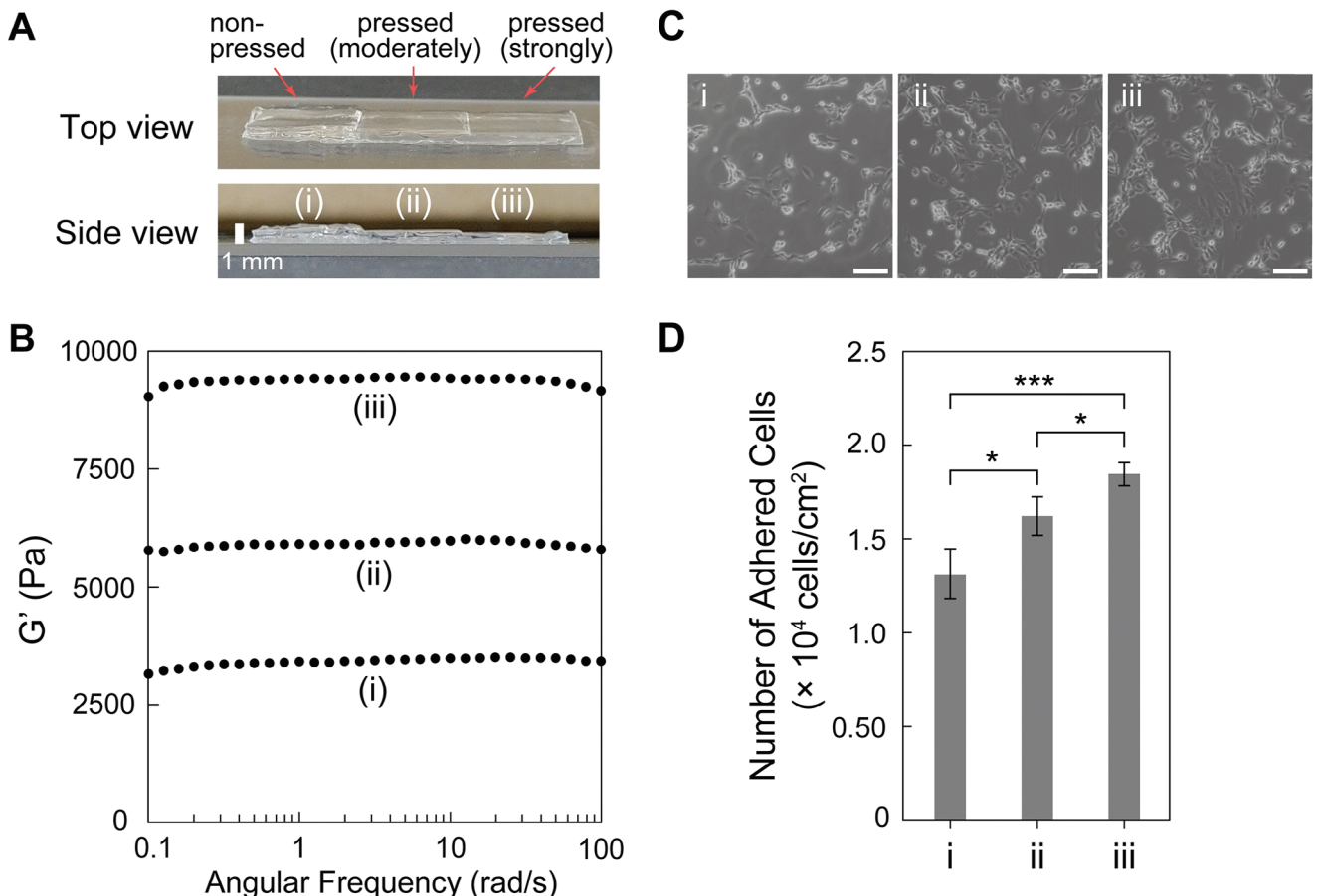


Figure 8. Preparation of the $x = 2$ hydrogel with different elastic moduli using the shape fix/memory properties and cell adhesion behavior onto the surfaces. A) Photographs of the hydrogel after the shape fix treatment: (i) non-pressed, (ii) moderately pressed, and (iii) strongly pressed regions. B) Plots of the G' of each region as a function of frequency (0.1–100 rad s $^{-1}$). C) Phase contrast images of the adhered NIT/3T3 cells on each region. Scale bar is 50 μ m. D) Number of the adhered cells calculated by WST-8 assay. Statistical analysis was performed using the t-test (N = 3). Error bars represent the standard deviation. * $p < 0.05$; *** $p < 0.005$.

4. Experimental Section

Materials: Fmoc-NH-SAL MBHA Resin, Fmoc-Arg(Pbf)-OH, Fmoc-Gly-OH, Fmoc-Asp(OtBu)-OH, Fmoc-Ser(tBu)-OH, 1-hydroxybenzotriazole (HOEt), and glycinate hydrochloride were purchased from Watanabe Chemical Industries, Ltd. (Japan). N, N'-diisopropylcarbodiimide (DHBA), tetramethylsilane (TMS), potassium carbonate, lipopolysaccharide (LPS), sodium nitrite, phosphoric acid, N-1-naphthylethylenediamine dihydrochloride (NED), and sulfanilamide (SUL) were purchased from FUJIFILM Wako Pure Chemical Co. (Japan). N, N-imethylformamide (DMF), piperidine, 2,2,2-trifluoroacetic acid (TFA), methanol, dichloromethane, triethylamine (TEA), diethyl ether, ammonium persulfate (APS), and sodium hydroxide were purchased from Nacalai Tesque, Inc. (Japan). Triisopropylsilane was purchased from Tokyo Chemical Industry Co., Ltd. (Japan). Methacrylic anhydride was purchased from Angene International Ltd. (China). 2-(3-(2-Methoxy-4-nitrophenyl)-2-(4-nitrophenyl)-2H-tetrazol-3-ium-5-yl)-5-sulfobenzenesulfonate sodium salt (WST-8) was purchased from Ambeed, Inc. (USA). 1-Methoxy-5-methylphenazinium methylsulfate (1-methoxy PMS) was purchased from Selleck Chemicals (USA). Special-grade solvents were used in all experiments unless otherwise specified. All the reagents were used as received.

Synthesis of N-acryloylglycinamide (NAGAm): NAGAm was synthesized according to the previous report.^[33]

¹H NMR (DMSO-*d*₆, TMS): δ 3.8 ppm (2H, —NHCH₂CO—), 5.6 ppm (1H, vinyl (*cis*), CH₂=CH—), 6.1 ppm (1H, vinyl (*trans*), CH₂=CH—), 6.3 ppm (1H, vinyl, CH₂=CH—), 7.0–7.5 ppm (2H, —CONH₂), and 8.3 ppm (1H, —NHCH₂CO—) (Figure S1, Supporting Information).

Synthesis of Cell-Binding Peptide Macromonomer: The peptide macromonomer was prepared via solid-phase peptide synthesis using Fmoc chemistry. The target sequence (methacryloyl-GGG-RGDS) was constructed on an Fmoc-NH-SAL MBHA resin using Fmoc-amino acid derivatives (3 equiv.), DIPC (3 equiv.), and HOEt (3 equiv.) in DMF for coupling (3 h), and piperidine (20 vol%)/DMF for Fmoc removal (30 min). A methacryloyl group was introduced at the N-terminus by treatment with methacryloyl anhydride (3 equiv.) and TEA (3 equiv.) in dichloromethane for 12 h. The peptide was cleaved from the resin by treatment with TFA/dichloromethane/TIS (v/v/v = 8.5/1/0.5) for 4 h. The obtained peptide (white solid) was purified by repeated precipitation from a methanol/diethyl ether system and subsequently identified using ¹H NMR and MALDI-TOF MS analyses.

MALDI-TOF MS (DHBA): [M+H]⁺ = 672.5 ([M+H]⁺_{theo}. = 672.3) (Figure S2A, Supporting Information).

¹H NMR (DMSO-*d*₆, TMS): δ 1.1–1.7 ppm (11H, —CH₂— : Arg-β, γ, —CH₃ : methacryloyl), 1.8–2.3 ppm (5H, H₂N—(C=NH)—NH— : guanidino group, Ser (—OH)), 2.6–3.0 ppm (4H, —CH₂ : Arg-δ, Asp-β), 3.7–3.9 ppm (10H, —CH₂— : Gly, Ser-β), 4.0–4.7 ppm (3H, —CH : Arg-α, Asp-α, Ser-α), 5.0–6.0 ppm (2H, *cis*, *trans* (CH₂ = C) : methacrylate),

and 7.0–8.5 ppm (7H , $-\text{CHNHCO}-$: amide) (Figure S2B, Supporting Information).

Preparation of Hydrogels Composed of RGDS Peptide-Grafted PNAGAm: Hydrogels composed of RGDS peptide-grafted PNAGAm were prepared by the radical copolymerization of NAGAm and the peptide macromonomer. The peptide grafting ratio was controlled by the feed composition used for polymerization. The peptide macromonomers, NAGAm and APS (1 mol%), were dissolved in water to a monomer concentration of 1 M. The aqueous solution was poured between two glass plates with a silicon spacer (thickness: 1 mm, AS ONE Co., Japan) and heated at 70 °C for 16 h. The hydrogels obtained were purified by repeated soaking in pure water.

Calculation of Changes in Swelling Ratio of the Hydrogels Depending on Temperature: The hydrogels were soaked in PBS (–) at various temperatures (T) for 1 h, and their surface areas (S_T) were measured. The surface area at 4 °C (S_4) was used as standard. Changes in the swelling ratio were determined using the following equation:

$$S_T/S_4 \times 100\% \quad (1)$$

Swelling Behaviors of the Hydrogels by Swelling/Shrinking Cycles: The hydrogels were repeatedly soaked in PBS (–) at 20 and 37 °C for 1 h, and their weights (W_{wet}) were measured. The hydrogels were then lyophilized to obtain their weights under dry conditions (W_{dry}). The swelling ratio at each temperature was determined using the following equation:

$$(W_{\text{wet}} - W_{\text{dry}})/W_{\text{dry}} \times 100\% \quad (2)$$

Cell Adhesion Experiments: The NIH/3T3 cells were purchased from the European Collection of Authenticated Cell Cultures (ECACC, UK). Cells were cultured in DMEM (FUJIFILM Wako Pure Chemical Co., Japan) containing 10% fetal bovine serum (FBS, Sigma-Aldrich, Co. LLC, USA) and 1% penicillin/streptomycin (PS, FUJIFILM Wako Pure Chemical Co., Japan). The hydrogels (1 × 1 cm) were placed into a 24-well polystyrene plate (Corning Inc., USA), soaked in PBS (–), and sterilized using ultraviolet light (254 nm) for 1.5 h. Then, 3.0×10^4 cells cm^{-2} of the cells were seeded onto the hydrogels at 37 °C for 16 h (5% CO_2) in serum medium or serum-free medium. Depending on the experiment, EDTA was added at a final concentration of 5 mM. The morphology of the adhered cells was observed using a phase-contrast microscope (CKX41; Olympus Co., Japan). The number of adhered cells was calculated using the WST-8 assay as follows: After culture, the medium was removed, and 450 μL of fresh DMEM without phenol red was added to the cell-adhered hydrogels. Then, 50 μL of solution for WST-8 assay, which is PBS (–) solution containing 5 mM of WST-8 and 200 μM of 1-methoxy PMS, was added to the hydrogels and incubated at 37 °C for 1 h. Two hundred microliters of the supernatants were poured into a 96-well polystyrene plate, and their absorbances at 450 nm were measured. The number of adhered cells was determined by comparison with a calibration curve.

Cell Proliferation Experiments: The cells were cultured in DMEM containing 10% FBS and 1% PS. The hydrogels (5 × 5 mm) were placed into 24-well polystyrene plates, soaked in PBS (–), and sterilized using ultraviolet light (254 nm) for 1.5 h. Then, the NIH/3T3 cells were seeded onto the hydrogels at a density of 2.0×10^3 cells cm^{-2} at 37 °C (5% CO_2). The number of adhered cells was calculated using the WST-8 assay after culturing for 1, 3, 5, 7, and 10 d.

NO Assay: RAW264.7 cells were purchased from ECACC (UK). The cells were cultured in RPMI1640 (FUJIFILM Wako Pure Chemical Co., Japan) containing 10% FBS and 1% PS. The hydrogels (4 × 4 mm) were placed in a 96-well polystyrene plate (Thermo Fisher Scientific Inc., USA) and sterilized using ultraviolet light (254 nm) for 1.5 h. Then, the cells were seeded onto the hydrogels at a density of 1.0×10^6 cells cm^{-2} at 37 °C for 24 h (5% CO_2) in serum medium without phenol red. The RAW264.7 cells were also cultured on tissue culture polystyrene (TCPS), with LPS (1 ng mL^{-1}) as the positive control and without LPS as the negative control. The NO production was calculated using the Griess reagent, which is an aqueous solution containing 0.05 w/v% NED, 0.5 w/v% SUL, and

2.5 v/v% phosphoric acid. After culture, 100 μL of the supernatants of the media were poured into a clean 96-well polystyrene plate. Then 100 μL of the Griess reagent was added to the supernatants and incubated at 37 °C for 20 min. The NO production was calculated by measuring the absorbance of the supernatants at 550 nm and comparing it with a calibration curve prepared using a standard solution of sodium nitrite.

Supporting Information

Supporting Information is available from the Wiley Online Library or from the author.

Acknowledgements

This work was supported by a Grant-in-Aid for Scientific Research (KAKENHI) (JP22K05232 to T.K.) from the Japan Society for the Promotion of Science (JSPS). This research was also supported by Grant-in-Aid for the Japan Prize Foundation (to S.N.), Lotte Research Promotion Grant (to S.N.), and All Doshisha Research Model “SDGs Research Project” (to T.K. and S.N.).

Conflict of Interest

The authors declare no conflict of interest.

Author Contributions

T.K. and S.N. conceived the study and designed the experiments. S.N. and T.Y. conducted the experiments. T.K. and S.N. obtained funding for the project and oversaw the research. S.N., T.Y., N.H., and T.K. wrote the manuscript. All the authors discussed the results and commented on the manuscript.

Data Availability Statement

The data that support the findings of this study are available from the corresponding author upon reasonable request.

Keywords

amino acid, cell scaffold, hydrogel, shape fix, shape memory, thermo-responsiveness

Received: September 23, 2023

Revised: January 14, 2024

Published online: February 9, 2024

- [1] R. Langer, J. P. Vacanti, *Science* **1993**, *260*, 920.
- [2] Y. Haraguchi, T. Shimizu, M. Yamato, T. Okano, *Stem Cells Transl. Med.* **2012**, *1*, 136.
- [3] G. L. Koons, M. Diba, A. G. Mikos, *Nat. Rev. Mater.* **2020**, *5*, 584.
- [4] Y. Zhao, S. Song, X. Ren, J. Zhang, Q. Lin, Y. Zhao, *Chem. Rev.* **2022**, *122*, 5604.
- [5] M. C. Catoira, L. Fusaro, D. Di Francesco, M. Ramella, F. Boccafoschi, *J. Mater. Sci. Mater. Med.* **2019**, *30*, 115.
- [6] D. Seliktar, *Science* **2012**, *336*, 1124.
- [7] T. Vermonden, R. Censi, W. E. Hennink, *Chem. Rev.* **2012**, *112*, 2853.

- [8] B. V. Slaughter, S. S. Khurshid, O. Z. Fisher, A. Khaderhosseini, N. A. Peppas, *Adv. Mater.* **2009**, *21*, 3307.
- [9] O. Wichterle, D. Lím, *Nature* **1960**, *185*, 117.
- [10] Q. Huang, Y. Zou, M. C. Arno, S. Chen, T. Wang, J. Gao, A. P. Dove, J. Du, *Chem. Soc. Rev.* **2017**, *46*, 6255.
- [11] C. D. Spicer, *Polym. Chem.* **2020**, *11*, 184.
- [12] D. D. Deligianni, N. D. Katsala, P. G. Koutsoukos, Y. F. Missirlis, *Biomaterials* **2000**, *22*, 87.
- [13] J. Y. Martin, Z. Schwartz, T. W. Hummert, D. M. Schraub, J. Simpson, J. Lankford Jr., D. D. Dean, D. L. Cochran, B. D. Boyan, *J. Biomed. Mater. Res.* **1995**, *29*, 389.
- [14] N. M. Alves, I. Pashkuleva, R. L. Reis, J. F. Mano, *Small* **2010**, *6*, 2208.
- [15] C. Xu, F. Yang, S. Wang, S. N. Ramakrishna, *J. Biomed. Mater. Res., Part A* **2004**, *71A*, 154.
- [16] G. R. Owen, J. Jackson, B. Chehroudi, H. Burt, D. M. Brunette, *Biomaterials* **2005**, *26*, 7447.
- [17] M. Padial-Molina, P. Galindo-Moreno, J. E. Fernández-Barbero, F. O'Valle, A. B. Jódar-Reyes, J. L. Ortega-Vinuesa, P. J. Ramón-Torregrosa, *Acta Biomater.* **2011**, *7*, 771.
- [18] R. Tzoneva, N. Faucheuix, T. Groth, *Biochim. Biophys. Acta Gen. Subj.* **2007**, *1770*, 1538.
- [19] T. G. van Kooten, J. M. Schakenraad, H. C. van der Mei, H. J. Busscher, *Biomaterials* **1992**, *13*, 897.
- [20] R. A. Gittens, L. Scheideler, F. Rupp, S. L. Hyzy, J. Geis-Gerstorfer, Z. Schwartz, B. D. Boyan, *Acta Biomater.* **2014**, *10*, 2907.
- [21] M. Tanaka, S. Kobayashi, D. Murakami, F. Aratsu, A. Kashiwazaki, T. Hoshiba, K. Fukushima, *Bull. Chem. Soc. Jpn.* **2019**, *92*, 2043.
- [22] S. Nishimura, M. Tanaka, *Bull. Chem. Soc. Jpn.* **2023**, *96*, 1052.
- [23] T. Yeung, P. C. Georges, L. A. Flanagan, B. Marg, M. Ortiz, M. Funaki, N. Zahir, W. Ming, V. Weaver, P. A. Janmey, *Cell. Motil. Cytoskeleton* **2005**, *60*, 24.
- [24] A. J. Engler, S. Sen, H. L. Sweeney, D. E. Discher, *Cell* **2006**, *126*, 677.
- [25] S. Nemir, H. N. Hayenga, J. L. West, *Biotechnol. Bioeng.* **2010**, *105*, 636.
- [26] R. H. Schmedlen, K. S. Masters, J. L. West, *Biomaterials* **2002**, *23*, 4325.
- [27] A. Banerjee, M. Arha, S. Choudhary, R. S. Ashton, S. R. Bhatia, D. V. Schaffer, R. S. Kane, *Biomaterials* **2009**, *30*, 4695.
- [28] H. Y. Yoshikawa, F. F. Rossetti, S. Kaufmann, T. Kaindl, J. Madsen, U. Engel, A. L. Lewis, S. P. Armes, M. Tanaka, *J. Am. Chem. Soc.* **2011**, *133*, 1367.
- [29] J. Thiele, Y. Ma, S. M. C. Bruekers, S. Ma, W. T. S. Huck, *Adv. Mater.* **2014**, *26*, 125.
- [30] S. Nishimura, T. Ueda, S. Kobayashi, M. Tanaka, *ACS Appl. Polym. Mater.* **2020**, *2*, 4790.
- [31] M. Boushta, P.-E. Colombo, S. Lenglet, S. Poujol, M. Vert, *J. Controlled Release* **2014**, *174*, 1.
- [32] Z. Xu, W. Liu, *Chem. Commun.* **2018**, *54*, 10540.
- [33] T. Koga, K. Tomimori, N. Higashi, *Macromol. Rapid Commun.* **2020**, *41*, 1900650.
- [34] U. Hersel, C. Dahmen, H. Kessler, *Biomaterials* **2003**, *24*, 4385.
- [35] Y. Ohmuro-Matsuyama, Y. Tatsu, *Angew. Chem., Int. Ed.* **2008**, *47*, 7527.
- [36] S. Petersen, J. M. Alonso, A. Specht, P. Duodu, M. Goeldner, A. del Campo, *Angew. Chem., Int. Ed.* **2008**, *47*, 3192.
- [37] X. He, J. Ma, E. Jabbari, *Langmuir* **2008**, *24*, 12508.
- [38] T. Koga, Y. Teraguchi, N. Higashi, *Trans. Mater. Res. Soc. Jpn.* **2012**, *37*, 533.
- [39] S. Nishimura, A. Hirata, Y. Taki, Y. Morita, N. Higashi, T. Koga, *Chem. Lett.* **2018**, *47*, 555.
- [40] S. Nishimura, N. Hokazono, Y. Taki, H. Motoda, Y. Morita, K. Yamamoto, N. Higashi, T. Koga, *ACS Appl. Mater. Interfaces* **2019**, *11*, 24577.
- [41] S. Nishimura, D. Sato, T. Koga, *Gels* **2023**, *9*, 829.
- [42] R. Pytela, M. D. Pierschbacher, S. Argraves, S. Suzuki, E. Ruoslahti, in *Methods in Enzymology*, Academic Press, **1987**, Vol. 144, pp. 475–489.
- [43] M. Busk, R. Pytela, D. Sheppard, *J. Biol. Chem.* **1992**, *267*, 5790.
- [44] C. Bogdan, *Nat. Immunol.* **2001**, *2*, 807.